

ROS generation and DNA damage with photo-inactivation mediated by silver nanoparticles in lung cancer cell line

 ISSN 1751-8741
 Received on 13th October 2015
 Revised 22nd March 2016
 Accepted on 27th April 2016
 E-First on 7th June 2016
 doi: 10.1049/iet-nbt.2015.0083
 www.ietdl.org

 Ahmed El-Hussein^{1,2,3} ✉, Michael R. Hamblin^{1,2,4}
¹Wellman Center for Photomedicine, Massachusetts General Hospital, Boston, MA 02114, USA

²Department of Dermatology, Harvard Medical School, Boston, MA 02115, USA

³Department of Laser Applications in Meteorology, Photochemistry, Photobiology and Agriculture, The National Institute of Laser Enhanced Science, Cairo University, Cairo, Egypt

⁴Harvard-MIT Division of Health Sciences and Technology, Harvard and Massachusetts Institute of Technology, Cambridge, MA 02139, USA

✉ E-mail: a.el-hussein@niles.edu.eg

Abstract: Lung cancer is considered one of the major health problems worldwide and the burden is even heavier in Africa. Nanomedicine is considered one of the most promising medical research applications nowadays. This is due to the unique physical and chemical properties of materials at the nanoscale. Silver nanoparticles have been extensively studied recently in many biomedical applications especially in cancer treatment, since they possess multifunctional effects that make these nanostructures ideal candidates for biomedical applications. AgNPs have been proved to have anti-tumour activity and the mode of cell death was shown to be apoptotic. The goal of the current work was to investigate the degree of DNA damage that may result from the usage of AgNPs as a photosensitiser in photo-inactivation and to evaluate the generation of reactive oxygen species (ROS) produced in the treatment. The results showed the occurrence of DNA damage in lung cancer cells (A549) through the generation of ROS shown by mitochondrial membrane potential changes.

1 Introduction

Lung cancer is considered one of the main causes of death all over the world, not only in western countries. It is believed to account for about 1.6 million deaths, 20% of the total cancer deaths [1]. The effect of this disease has increased lately in Africa due to the tobacco epidemic that has resulted in the vast dispersion of this disease [2]. According to the international agency for research on cancer (IARC), smoking alone causes about 65% of lung cancers. Their estimation forecasts the appearance of 1.8 million new cases in 2012 and about 60% of this number is in the less developed countries as shown in Table 1 [3].

About 85% of lung cancer patients are diagnosed with either metastasis or locally advanced tumours or both. Surgery could be one of the first approaches, but unfortunately it is only indicated for 15% of the patients. Bronchoscopic therapy could be the quickest choice and even the only possible choice in treating superficial tumours that are found intraluminally and for the

treatment of tumours in the main airways as it can cause a rapid symptomatic relief for those patients and hence their overall conditions. This can give the chance for the chemotherapy and/or radiotherapy treatments to maintain or improve local disease [4]. The blockage of the main airways by large tumours is the main cause of deaths due to dyspnoea and obstructive pneumonia. However, this approach fails with deep tumours and those who are extension distal to the segmental bronchi. The term 'tumour resistance' is very familiar since a high proportion of lung cancers were found to be resistant to conventional combined therapies that eventually cannot compete with tumour recurrence or progression [5]. Thus, there is an urgent need to introduce a new approach such as photodynamic therapy (PDT) for the treatment of lung cancer disease. For more than a quarter of a century, PDT has been actively applied in the oncology field to provide a significant clinical applications in cancer treatment or skin-related diseases. PDT has selectivity for tumours due to the high photosensitiser

Table 1 Incidence prevalence and deaths worldwide in 2012 for lung cancer [3]

Estimated numbers (thousands)	Men		Women		Both sexes	
	Cases	Deaths	Cases	Deaths	Cases	Deaths
worldwide	1242	1099	583	491	1825	1590
developed regions	490	417	268	210	758	627
less developed regions	751	682	315	281	1066	963
WHO Africa region (AFRO)	12	11	6	6	18	16
WHO Americas region (PAHO)	178	149	146	113	324	262
WHO East Mediterranean region	26	23	7	6	33	29
WHO Europe region (EURO)	323	283	126	105	449	388
WHO South-East Asia region	116	104	46	42	162	146
WHO western pacific region	588	528	251	220	839	748
IARC membership (24 countries)	514	438	279	219	794	657
United States of America	112	92	102	76	214	168
China	459	422	193	175	653	597
India	54	49	17	15	70	64
European Union (EU-28)	214	186	99	82	313	268

(PS) affinity to tumour tissue, the local illumination of the tumour area, and finally to the good regeneration of normal tissue after applying PDT [6]. Yet PDT has its own limitations including the penetration limit of the light itself, long-lasting skin sensitivity and the sub-therapeutic level of PS accumulated in the cancerous tissue. These drawbacks have hindered the development of PDT in favour of other conventional approaches. Recently, the development of new PS, improved light sources as well as drug delivery approaches and the activation of the host immune response are all factors that can play a role in increasing the likelihood of PDT to be applied either alone or combined with other therapies in the effective treatment of cancer.

Recently, silver nanoparticles (AgNPs) have received increased interest, especially after being shown in a previously published work to have the possibility of using them as PS. Generally, AgNPs have distinctive characteristics and wide applications from ink-jet printing to antimicrobial applications, and have been found to affect both neurons and undifferentiated cells [7–9]. The aim of the present paper was to study closely how AgNPs mediate their cytotoxicity and if they affect the cellular DNA or not. Hence, a better understanding of their mechanism of action could help the future development of such nanostructures and their applications in PDT alone and/or with combined chemotherapy.

2 Materials and methods

Lung cancer (A549) cell line came from the American Type Cell Culture (ATCC; Manassas, VA, USA) (ATCC HTB-53). Cell Culture growth media were manufactured by Gibco (Thermo Fisher Scientific, Waltham, MA, USA). A549 cancer cells were cultured in Roswell Park Memorial Institute media that was supplemented with 10% foetal bovine serum and 1% penicillin/streptomycin/fungizone (GE Healthcare Bio-Sciences Corp., Piscataway, NJ, USA) with 5% CO₂ and at 37°C. On reaching confluency, they were washed with Hank's balanced salt solution (HBSS; Thermo Fisher Scientific) and trypsinised by TrypLE™ Express (Gibco®; Thermo Fisher Scientific). Cells were then seeded with a concentration of 3×10^5 in culture dishes of 3.3 cm diameter where they were left 4 h to attach. Then, 3.23 mg/ml of AgNPs (final concentration) was introduced to those attached cells and left overnight. Laser irradiations with 20 J/cm² were performed in the dark through an optical fibre at room temperature, where the laser spot size covered exactly the cell monolayer in the culture plates. The parameters of the used laser were those summarised in our previous work [10].

The AgNPs were synthesised at the Institute of Photonic Technology in Jena, Germany. The main characteristics of the used AgNPs have been described in an earlier work [10], where the stock solution was at a concentration 80.884 mg/ml.

Cellular assays measurements were done on a Victor3 Multi-label Plate Reader (PerkinElmer Inc., Waltham, MA, USA).

The AgNPs that were used in the current study have an absorption peak at 630 nm which is not in the usual absorption spectrum of Ag. Laser-induced breakdown spectroscopic (LIBS) technique was used to provide more validation about the identity of the used NPs. It is an elemental quasi-invasive tool with minimal sample preparation [11]. The setup has been described before by El-Hussein *et al.* [12]. Briefly, two sample droplets were put on an ashless filter paper and left for sample spreading for about 10–15 min. The excitation source was a Q-switched neodymium-doped yttrium aluminium garnet laser (BRIO, Quantel, France) at its fundamental wavelength ($\lambda = 1064$ nm), having a pulse energy of 65 mJ and a pulse width of 5 ns at 10 Hz repetition rate. A 10 cm plano-convex lens was used to focus the laser beam on the sample that resulted in an irradiance of several megawatts in magnitude that was capable of producing laser-induced plasma. The emitted plasma is considered as the elemental finger-print of the sample under test and the plasma emission was driven via an optical fibre to an echelle spectrometer (Mechelle 7500, multichannel, Sweden) coupled to an Intensified charged coupled device camera (DiCAM-PRO, PCO-computer optics, Germany) with its appropriate software for further analysis.

The current experiment had the setup where cell cultures were divided into four study groups: the first one was used as a control where cells were cultured normally in media and with 5% CO₂ supplement; the second group was treated similarly, but irradiated with a light dose of 20 J/cm²; the third group was treated as group one, but with the addition of 3.23 mg/ml AgNPs; and the last group was the PDT group as the cells of this group had both 3.23 mg/ml AgNPs and laser irradiation at 20 J/cm².

Intracellular reactive oxygen species (ROS) was estimated in all the four experimental groups where 1×10^5 of A549 cells were plated in 96 well plates accordingly and washed with Phosphate buffer saline twice. The cells were then incubated with 10 μ M 5-(and-6)-chloromethyl-2, 7-dichlorodihydrofluorescein diacetate acetyl ester (CM-H2DCFDA) dye at 37 °C for 1 h. Thereafter, the fluorescence intensity was measured at 530 nm via the plate reader.

This dye is non-fluorescent when chemically reduced, but after cellular oxidation and removal of acetate groups by cellular esterases it becomes fluorescent. CM-H2DCFDA is a derivative of DCF-DA, but with an additional thiol reactive chloromethyl group, which enhances the ability of the compound to bind to intracellular components, thereby prolonging the dye's cellular retention.

Moreover, the mitochondrial membrane potential, $\Delta\Psi_m$ was investigated. This parameter is important since it can be used as a cell health indicator. JC-1 mitochondrial membrane potential assay kit (Cayman chemical, MI, USA), Zeiss confocal microscope, and the fluorescence plate reader were used in the current research for such purpose. This method relies on the lipophilicity of JC-1 and its cationic nature that can enter the mitochondria in a selective manner, where it forms a complex called J-aggregates whose colour is red in healthy mitochondria, but reversibly changes its colour to green when the mitochondrial membrane potential is low. The ratio of green to red fluorescence depends only on the membrane potential and not on other factors such as mitochondrial size, shape, and density, which may influence single-component fluorescence signals. In apoptotic or unhealthy cells with low ($\Delta\Psi_m$), JC-1 remains in the monomeric form, which shows only green fluorescence [13].

The cells from the four experimental groups were plated in 96 well plates at 1×10^5 cells/ml and left for 8–12 h. About 100 μ l/ml of JC-1 staining solution was added to each well and mixed gently. The plates were then incubated for 20–40 min at 37 °C and 5% CO₂. The plates were then read using excitation/emission 540/570 nm for healthy cells or 485/535 nm for apoptotic conditions and imaged using Zeiss multi-laser confocal microscope. Healthy cells, JC-1 forms J-aggregates which have strong fluorescence intensity at 595 nm \times 535 nm excitation wavelength. While JC-1 in apoptotic cells exists as monomers that have strong fluorescence intensity at 535 nm \times 485 nm excitation wavelength. The ratio of fluorescent intensity of J-aggregates to fluorescent intensity of monomers is used as an indicator of cell health.

Comet assay (single cell gel electrophoresis) was used for the estimation of DNA damage that may be caused through the usage of AgNPs as a PS in PDT treatment of A549 cell line. The assay was explained in detail in an earlier work [14]. Briefly cells from each experimental group were trypsinised and suspended in low melting point agarose and cast into a gel film. After the agarose polymerised, cells were lysed overnight in fresh lysis buffer. The slides were placed in alkaline solution (0.3 M NaOH; 1 mM Ethylenediaminetetraacetic acid) for 40 min at 4 °C prior to electrophoresis at 25 V for 30 min at 4 °C and pH 12.7. Neutralisation was done for 2 h in 0.4 M Tris at pH 7.5. Post-staining with 1 μ g/ml 4',6-diamidino-2-phenylindole (DAPI; a fluorescent dye which binds to DNA). The visual assessment of the relative tail intensity using a Zeiss upright microscope associated with a Charged coupled device camera was done, by sorting 100 comets into classes from 0 (no detectable tail) to 4 (large tail, minimal head), giving an overall damage score of 0–400.

All sets of experiments were repeated four times with duplicate replications of each assay. Origin pro 8 was used as software for performing one way statistical analysis for means, standard deviations, and standard error values. *P*-values were designated for

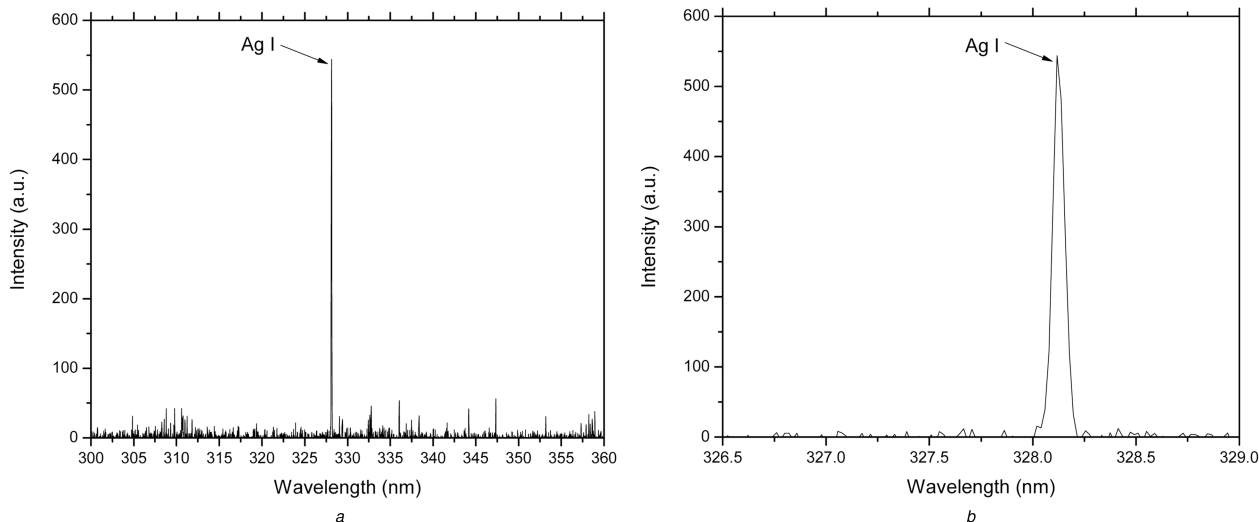


Fig. 1 LIBS spectra showing the Ag spectral line at 328.2 nm with high intensity (higher resolution at B) for the synthesised NPs confirming the presence of Ag

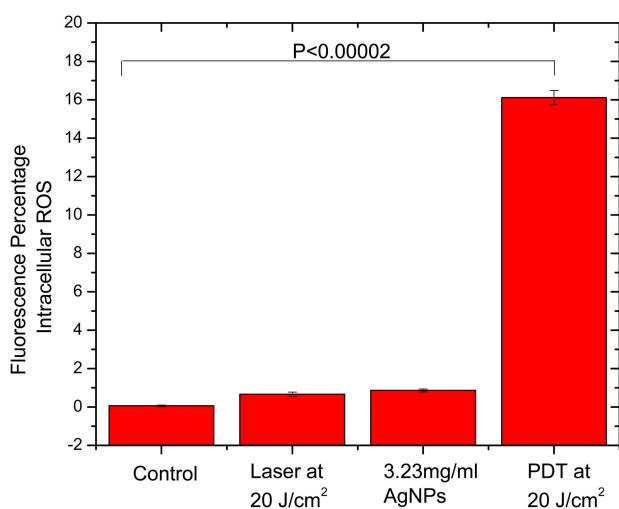


Fig. 2 Different experimental groups stained with fluorescent 5-(and-6)-chloromethyl-2,7 dichlorodihydrofluorescein diacetate acetyl ester showing the generation of intracellular ROS in the PDT group with significance $p < 0.0002$ compared with the control group

the statistical significance between the control groups and the PDT treated groups using AgNPs.

3 Results and discussion

LIBS technique confirmed the elemental constituent of the synthesised NPs to be Ag. According to the National Institute of Standards and Technology, the spectral line which is at 328.2 nm is characteristic of elemental Ag as shown in Fig. 1.

The current study showed that the cytotoxicity produced PDT mediated by AgNPs was found to be due to the generation of intracellular ROS as seen in Fig. 2. However, the dosage and exposure time need to be further studied to elucidate the complexity and details. It is apparent from the figure that the AgNPs alone and the laser irradiation alone resulted in a small non-significant increase in ROS compared with the control group. On the other hand, the PDT group generated a large increase in intracellular ROS compared with the control group with $p < 0.00002$.

One interesting question that remains to be answered is what is the exact mechanism of action of the light activation of AgNPs. Traditional PDT works by reactions arising from the triplet state of a PS. The long-lived triplet state can undergo energy transfer to ground state triplet oxygen to form the ROS, singlet oxygen [6]. Since AgNPs do not have a long-lived triplet state, this mechanism cannot apply in the present paper. However, the PS triplet state can

also carry out electron transfer processes that also result in the generation of ROS [15]. It is possible that AgNPs can carry out electron transfer reactions from the conduction band electrons that form surface plasmon resonances when excited by light [16]. Alternative mechanisms include the absorbance of light producing localised photothermal effects in the close vicinity of the AgNPs [17], and the possible light-induced release of Ag⁺ ions from the AgNPs that could interact with specific proteins [18].

Many studies have reported the generation of ROS in many cell lines due to the introduction of NPs; see for instance reports by Mukherjee *et al.* [19] and Bhattacharya *et al.* [20]. AgNPs are one of the most prominent candidates in nanomedicine since they are believed to have a big role in causing cellular oxidative stress which consequently results in ROS production. The cytotoxicity of AgNPs has been shown by many research centres to be both size- and shape-dependent. Carlson *et al.* [21] concluded that AgNPs induced size-dependent cytotoxicity, i.e. smaller NPs with a size (15–30 nm) induced higher cell death via oxidative stress. Kim *et al.* [22] reached a similar conclusion in his work where he found the cytotoxic effects of AgNPs to MC3T3-E1 cells (via apoptosis) and PC12 cells (via necrotic cell death) were both size and dose-dependent (10 nm compared with 100 nm). Even the well-known bactericidal effect of AgNPs has been found to be size-dependent, since NPs whose diameters are in the range of 10 nm show a direct interaction with the bacteria [23].

As the size of the AgNPs decreases, their exposed surface area (that can be involved in the biochemical interactions with the cells) is increased, and hence their cellular effects are elevated by several folds. The size of the AgNPs used in the current study was around 27 nm and with a spherical shape [10] that rendered them efficient in interacting with cells.

Mitochondria are the main energy source of the cell. Mitochondria use electrochemical proton motive force (Δp) that is produced by oxygen reduction via the respiratory electron transport chain to eventually generate Adenosine triphosphate. As shown by the Nernst equation, the total force driving protons into the mitochondria (i.e. Δp) is a combination of both the mitochondrial membrane potential ($\Delta\psi_m$, a charge or electrical gradient) and the mitochondrial pH gradient (Δp_{Hm} , an H⁺ chemical or concentration gradient) [13]. A positive correlation has been reported between ROS and mitochondrial membrane potential ($\Delta\psi_m$) in healthy undamaged cells. It is well known that mitochondria can produce more ROS at higher membrane potential. The work that has been done on *Drosophila melanogaster* revealed that a small decrease in mitochondrial membrane potential ($\Delta\psi_m$) corresponds to a significant decrease in ROS production (can reach to 70% ROS reduction) [24].

However, the opposite effect is also well known, where ROS generation is associated with lower (not higher) mitochondrial membrane potential. This phenomenon has been called

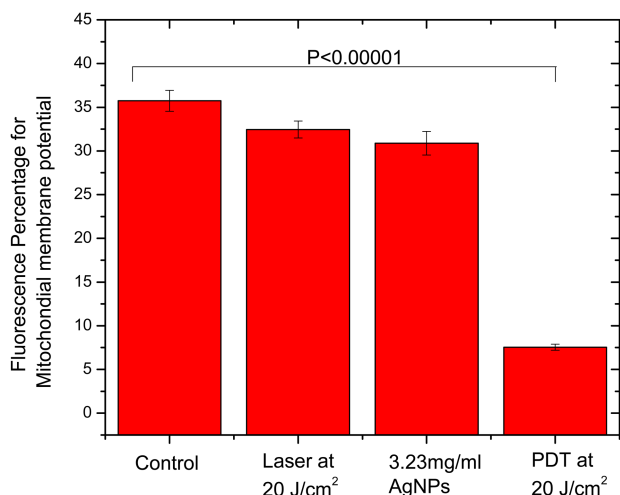


Fig. 3 Different experimental groups stained with JC-1 fluorescent dye showing the significant change in the mitochondrial membrane potential in the PDT group compared with the control group where $p < 0.0001$

'mitochondrial ROS-induced ROS release' [25]. The exposure to excessive oxidative stress results in an increase in intracellular ROS that reaches a threshold level that triggers the opening of the mitochondrial permeability transition pores (mPTPs). In turn, this leads to the collapse of the mitochondrial membrane potential and a further increased ROS generation by the electron transfer chain.

A significant decrease in the mitochondrial membrane potential ($\Delta\Psi_m$) in the PDT group was observed when compared with the control group ($p < 0.00001$) as shown in Fig. 3 displaying the changes in ($\Delta\Psi_m$) in the different experimental groups.

Confocal microscopic imaging added strength to the above results by showing the green monomeric form of the JC-1 fluorescent dye in the case of the PDT experimental group where the other experimental groups have shown the healthy red J-aggregates as a result of the complex formation in the mitochondria as shown in Fig. 4.

Despite the existence of many pathways for the generation of ROS, the main mechanism is the mitochondrial generation of ROS pathway via the electron transport chain [26]. The large increase in ROS seen in the cells is partly due to the ROS produced by laser irradiation of the AgNPs that damage the mitochondria. This mitochondrial damage eventually leads to opening of the mPTP, followed by depolarisation of the mitochondrial membrane potential and further additional generation of ROS. At higher ROS levels, longer mPTP openings may release an ROS burst leading to destruction of mitochondria, and if propagated from mitochondrion to mitochondrion, of the cell itself. The destructive function of ROS-induced ROS release may serve a physiological role by removal of unwanted cells or damaged mitochondria [27].

Studying the DNA damage that may be caused by AgNPs in the PDT treatment of A549 cells using the comet assay showed a significant DNA fragmentation in the PDT group compared with the control group with $p < 0.0001$ as shown in Fig. 5.

There is not yet a consensus about the pathway of the mitochondrial ROS generation in the cytotoxicity mediated by AgNPs either in the dark, or when activated by light. There might be other cell organelles and pathways that could be involved in these reactions with other mechanisms of increased oxidative stress after intracellular ROS generation and DNA fragmentation. One proposed mechanism could be proposed from the overall data and from other recent research [28] that the Ag⁺ ions which were generated after laser irradiation of the AgNPs can interfere with DNA replication and cause the induction of ROS and eventually cell death. There are two main pathways of apoptosis by PDT, which are extrinsic (cytoplasmic) or intrinsic (mitochondrial pathway). The latter pathway is initiated when the mitochondrial membrane becomes more permeable and causes release of cytochrome C into the cytosol. The released cytochrome C interacts with apoptotic protease activating factor and dATP to form the apoptosome. The latter leads to the activation of caspase-9

that in turn activates caspase-3, where it activates the rest of caspase cascade. Eventually, the process ends by the cleavage of poly Adenosine diphosphate-ribose polymerase and DNA fragmentation [29].

In our previous work, we found the zeta potential of the used AgNPs [10] to have a very small value. This may result in aggregation of the AgNPs on protein adsorption on their surface [30, 31]. Zeta potential can be defined as the voltage potential difference between the dispersion medium and the stationary layer of the liquid attached to the dispersed medium. It determines the electro-kinetic potential of any colloidal system as it determines the stability of such dispersions. The magnitude of the zeta potential indicates the degree of electrostatic repulsion between adjacent, similarly charged particles. Zeta potential is a key indicator of the stability of colloidal dispersions. A high zeta potential value for small molecules and particles means a stable colloidal system as the dispersion will resist aggregation. On the other hand, when the potential is small, attractive forces may exceed this repulsion and the dispersion may be unstable and aggregate. Lynch *et al.* [31] have proposed in their work that the biological responses in biological colloidal systems where NPs are involved are dependent on the amount and presentation of the outer layer of adsorbed proteins on the surface (protein corona) rather than on the particles themselves. Cho *et al.* [32] have discussed the effect of zeta potential and the NP size as a crucial factor on their agglomeration and hence in inducing cellular response, and they specified a threshold size limit of 50 nm. The current work showed no genotoxicity of the AgNPs by itself, but after light absorption they generated ROS (through the observed decreased cell viability and increased fluorescent signal on using CM-H2DCFDA with the change of mitochondrial membrane potential that can lead to a serious reactions that eventually lead (in the absence of antioxidant protection) to DNA damage and apoptosis [33]. It should be noted that the comet assay can detect DNA damage caused by cleavage of DNA in cells occurring as the final end-stage of apoptosis, and can also detect DNA damage caused by direct chemical attack on the polynucleotide chains by such species as ROS [34]. The terminal deoxynucleotidyl transferase mediated dUTP nick end labelling (Terminal deoxynucleotidyl transferase dUTP nick end labeling assay) can be used to distinguish between these two different types of DNA fragmentation. ROS can be induced via other organelles and pathways such as Golgi apparatus, endosomes, and lysosomes after cellular exposure to other types of NPs [35].

NPs can be specifically accumulated in tumours and malignant cells rather than normal cells and tissues, hence providing therapeutic specificity. This is due to what is known as the enhanced permeability and retention effect where the blood vessels around tumour cells are porous and leaky so that NPs are retained in these cells. There are other factors such as lower pH found in tumours that enhance the cellular uptake and poor lymphatic drainage in tumour cells that would help the NPs accumulation as well. Moreover, this leaky vasculature favours accumulation of lipophilic compounds with which NPs could be functionalised (or even be combined with other lipophilic PSs that could have additive or synergistic PDT effects) or for improving drug delivery vehicles. The unique optical and chemical properties of many NPs such as gold render them a promising tool for better imaging and early diagnosis, where early and successful tumour detection is considered the main factor that controls patients' survival rate. At the same time, little is known so far about the toxicity and health hazards of NPs, and their possible harmful outcomes on human and/or animal health should not be overlooked. This concern comes from the results or recent studies that showed the serious impacts on the appearance of cardiac events by the daily exposure to NPs for short and long terms as well as the potential of general and localised air, water pollution incidence [36].

4 Conclusions

The current work aimed to investigate how AgNPs can induce cytotoxicity in A549 cell line. The study revealed that after PDT treatment, these NPs induced the generation of intracellular ROS with the change of the mitochondrial membrane potential. Studying

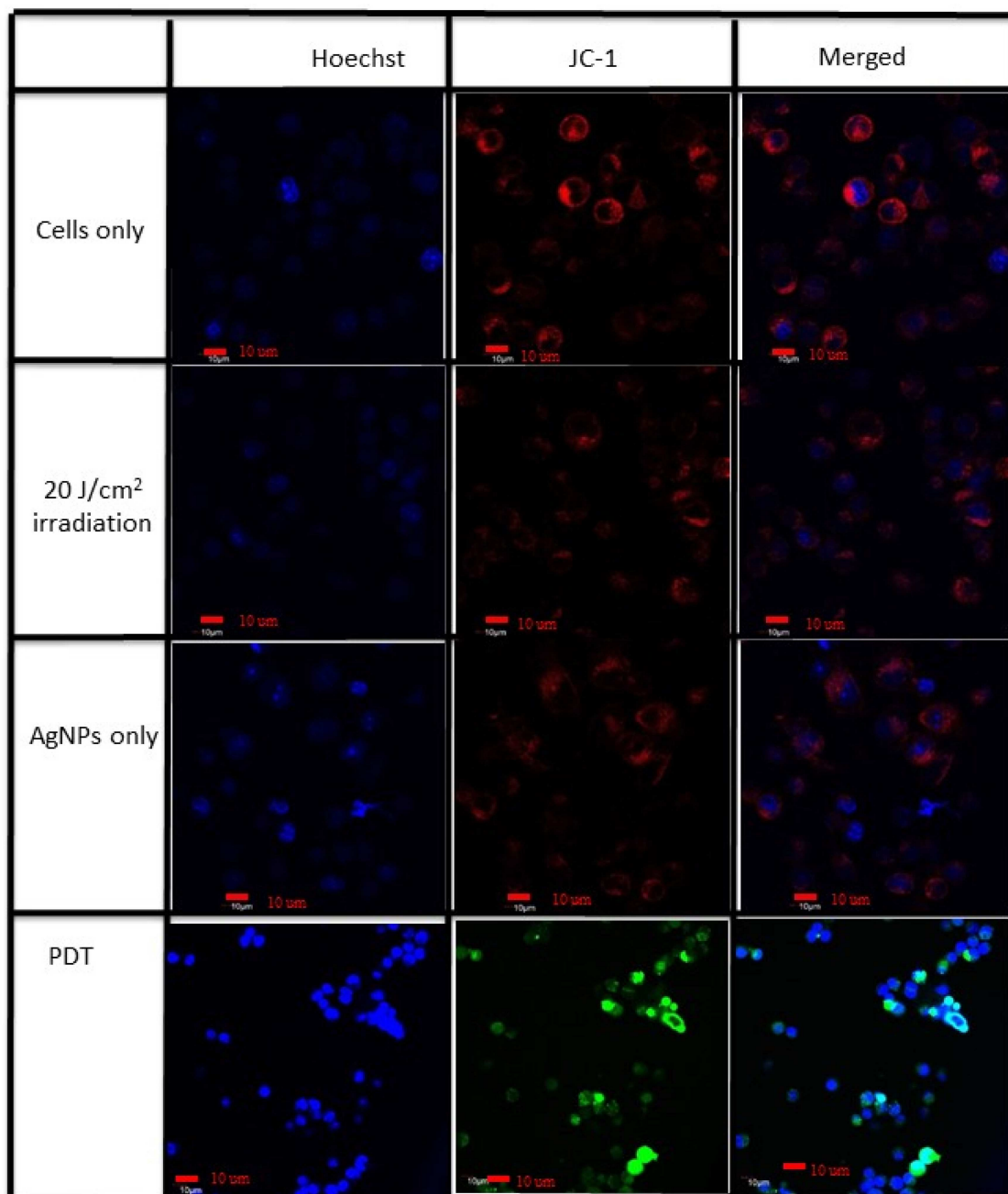


Fig. 4 Confocal imaging of control, AgNPs only and laser of 20 J/cm² only show the healthy red J-aggregates in the mitochondria while the PDT group shows the green J-monomer due to the decreased mitochondrial membrane potential

the occurrence of DNA damage in the PDT experimental group confirmed that these intracellular ROS could in turn induce DNA fragmentation and hence cell death through apoptosis. These effects have been significantly shown only in the PDT group as neither the AgNPs alone nor could the laser alone induce such observed effects. Yet there is still a need for future and extensive work to study the role of other possible organelles candidates in the ROS generation and hence genotoxicity.

5 Acknowledgment

Acknowledgements are extended to Professor Wolfgang Fritzsche and his research team, Nano Biophotonics Department, Institute of Photonic Technology (IPHT), Jena, Germany for the synthesis and supply of AgNPs.

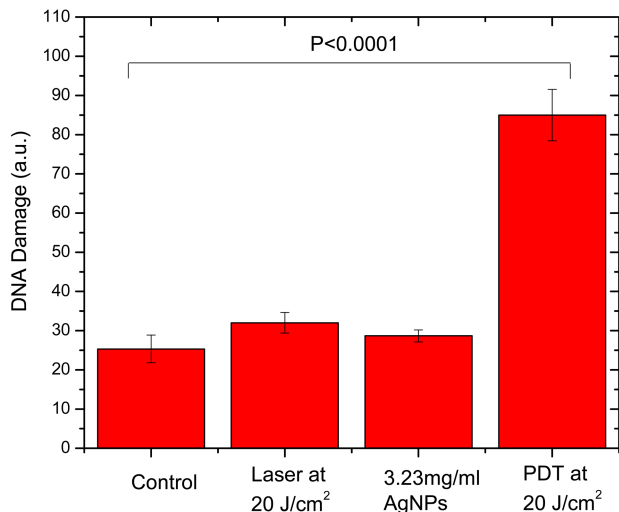


Fig. 5 Comet assay identifying the DNA damage for the four experimental groups of A549 cancer cells, showing significant DNA damage after PDT treatment compared with the control group ($p < 0.0001$)

6 References

- [1] El Hussein, A., Mfouo-Tynga, I., Abdel-Harith, M., et al.: 'Comparative study between the photodynamic ability of gold and silver nanoparticles in mediating cell death in breast and lung cancer cell lines', *J. Photochem. Photobiol. B*, 2015, **153**, pp. 67–75
- [2] Jemal, A., Bray, F., Center, M.M., et al.: 'Global cancer statistics', *CA Cancer J. Clin.*, 2011, **61**, pp. 69–90
- [3] WHO 2015. Available at <http://www.globocan.iarc.fr/old/FactSheets/cancers/lung-new.asp>
- [4] Kato, H.: 'Photodynamic therapy for lung cancer – a review of 19 years' experience', *J. Photochem. Photobiol. B*, 1998, **42**, pp. 96–99
- [5] Simone, C.B., Friedberg, J.S., Glatstein, E., et al.: 'Photodynamic therapy for the treatment of non-small cell lung cancer', *J. Thorac. Dis.*, 2012, **4**, pp. 63–75
- [6] Agostinis, P., Berg, K., Cengel, K.A., et al.: 'Photodynamic therapy of cancer: an update', *CA Cancer J. Clin.*, 2011, **61**, (4), pp. 250–281
- [7] Su, J., Zhang, J., Liu, L., et al.: 'Exploring feasibility of multicolored CdTe quantum dots for in vitro and in vivo fluorescent imaging', *J. Nanosci. Nanotechnol.*, 2008, **8**, pp. 1174–1177
- [8] Marambio-Jones, C., Hoek, E.M.V.: 'A review of the antibacterial effects of silver nanomaterials and potential implications for human health and the environment', *J. Nanopart. Res.*, 2010, **12**, pp. 1531–1551
- [9] Barbasz, A., Oćwieja, M., Barbasz, J.: 'Cytotoxic activity of highly purified silver nanoparticles sol against cells of human immune system', *Appl. Biochem. Biotechnol.*, 2015, **176**, pp. 817–834
- [10] Mfouo-Tynga, I., Hussein, A., Harith, M., et al.: 'Photodynamic ability of silver nanoparticles in inducing cytotoxic effects in breast and lung cancer cell lines', *Int. J. Nanomed.*, 2014, **9**, pp. 3771–3780
- [11] El-Hussein, A., Kassem, A.K., Ismail, H., et al.: 'Exploiting LIBS as a spectrochemical analytical technique in diagnosis of some types of human malignancy', *Talanta*, 2010, **82**, pp. 495–501
- [12] El Hussein, A., Marzouk, A., Harith, M.: 'Discrimination between different crude oil grades using laser induced break down spectroscopy', *Spectrochim. Acta B*, 2015, **113**, pp. 93–99
- [13] Perry, S.W., Norman, J.P., Barbieri, J., et al.: 'Mitochondrial membrane potential probes and the proton gradient: a practical usage guide', *Biotechniques*, 2011, **50**, pp. 98–115
- [14] El-Hussein, A., Harith, M., Abrahamse, H.: 'Assessment of DNA damage after photodynamic therapy using a metalphthalocyanine photosensitizer', *Int. J. Photoenergy*, 2012, (2012), doi: 10.1155/2012/281068
- [15] Huang, L., St Denis, T.G., Xuan, Y., et al.: 'Paradoxical potentiation of methylene blue-mediated antimicrobial photodynamic inactivation by sodium azide: role of ambient oxygen and azide radicals', *Free Radic. Biol. Med.*, 2012, **53**, (11), pp. 2062–2071
- [16] Zhang, W., Li, Y., Niu, J., Chen, Y., et al.: 'Photogeneration of reactive oxygen species on uncoated silver, gold, nickel, and silicon nanoparticles and their antibacterial effects', *Langmuir*, 2013, **29**, (15), pp. 4647–4651
- [17] Thompson, E.A., Graham, E., MacNeill, C.M., et al.: 'Differential response of MCF7, MDA-MB-231, and MCF 10A cells to hyperthermia, silver nanoparticles and silver nanoparticle-induced photothermal therapy', *Int. J. Hyperth.*, 2014, **30**, (5), pp. 312–323
- [18] Jin, Y., Dai, Z., Liu, F., et al.: 'Bactericidal mechanisms of Ag(2) O/TNPs under both dark and light conditions', *Water Res.*, 2013, **47**, (5), pp. 1837–1847
- [19] Mukherjee, S.P., Lyng, F.M., Garcia, A., et al.: 'Mechanistic studies of in vitro cytotoxicity of poly (amidoamine) dendrimers in mammalian cells', *Toxicol. Appl. Pharmacol.*, 2010, **248**, pp. 259–268
- [20] Bhattacharya, K., Pratap, C., Nahaa, C., et al.: 'Reactive oxygen species mediated DNA damage in human lung alveolar epithelial (A549) cells from exposure to non-cytotoxic MFI-type zeolite nanoparticles', *Toxicol. Lett.*, 2012, **215**, pp. 151–160
- [21] Carlson, C., Hussain, S.M., Schrand, A.M., et al.: 'Unique cellular interaction of silver nanoparticles: size-dependent generation of reactive oxygen species', *J. Phys. Chem. B*, 2008, **112**, pp. 13608–13619
- [22] Kim, T.H., Kim, M., Park, H.S., et al.: 'Size-dependent cellular toxicity of silver nanoparticles', *J. Biomed. Mater. Res. A*, 2012, **100**, pp. 1033–1043
- [23] Morones, J.R., Elechiguerra, J.L., Camacho, A., et al.: 'The bactericidal effect of silver nanoparticles', *J. Nanotechnol.*, 2005, **16**, p. 2346
- [24] Suski, J.M., Lebedzinska, M., Bonora, M., et al.: 'Relation between mitochondrial membrane potential and ROS formation', *Methods Mol. Biol.*, 2012, **810**, pp. 183–205
- [25] Zorov, D.B., Juhaszova, M., Sollott, S.J.: 'Mitochondrial ROS-induced ROS release: an update and review', *Biochim. Biophys. Acta*, 2006, **1757**, (5-6), pp. 509–517
- [26] McLennan, H.R., Esposti, M.D.: 'The contribution of mitochondrial respiratory complexes to the production of reactive oxygen species', *J. Bioenerg. Biomembr.*, 2000, **32**, pp. 153–162
- [27] Zorov, D.B., Juhaszova, M., Sollott, S.J.: 'Mitochondrial reactive oxygen species (ROS) and ROS-induced ROS release', *Physiol. Rev.*, 2014, **94**, (3), pp. 909–950
- [28] Kreuter, J., Gelperina, S.: 'Use of nanoparticles for cerebral cancer', *Tumori*, 2008, **94**, pp. 271–277
- [29] Cai, J., Yang, J., Jones, D.P.: 'Mitochondrial control of apoptosis: the role of cytochrome c', *Biochim. Biophys. Bioenerg.*, 1998, **1366**, pp. 139–149
- [30] Gray, J.J.: 'The interaction of proteins with solid surfaces', *Curr. Opin. Struct. Biol.*, 2004, **14**, pp. 110–115
- [31] Lynch, I., Cedervall, T., Lundqvist, M., et al.: 'The nanoparticle-protein complex as a biological entity: a complex fluids and surface science challenge for the 21st century', *Adv. Colloid Interface Sci.*, 2007, **134**, pp. 167–174
- [32] Cho, E.C., Zhang, Q., Xia, Y.: 'The effect of sedimentation and diffusion on cellular uptake of gold nanoparticles', *Nat. Nanotechnol.*, 2011, **6**, pp. 385–391
- [33] Halliwell, B., Whiteman, M.: 'Measuring reactive species and oxidative damage in vivo and in cell culture: how should you do it and what do the results mean?', *Br. J. Pharmacol.*, 2004, **142**, pp. 231–255
- [34] Wada, S., Khoa, T.V., Kobayashi, Y., et al.: 'Detection of radiation-induced apoptosis using the comet assay', *J. Vet. Med. Sci.*, 2003, **65**, (11), pp. 1161–1166
- [35] Jiang, Z., Hu, Z., Zeng, L., et al.: 'The role of the Golgi apparatus in oxidative stress: is this organelle less significant than mitochondria?', *Free Radic. Biol. Med.*, 2011, **50**, pp. 907–917
- [36] Gwinn, M.R., Vallyathan, V.: 'Nanoparticles: health effects – pros and cons', *Environ. Health*, 2006, **114**, pp. 1818–1825